

Reptational dynamics of a polymer chain is stable against kinematic disorder

L. Schäfer^{1,a}, A. Baumgärtner², and U. Ebert³

¹ Fachbereich Physik, Universität Essen, 45117 Essen, Germany

² Institut für Festkörperforschung and Forum Modellierung, Forschungszentrum Jülich, 52425 Jülich, Germany

³ Center voor Wiskunde en Informatica, Cluster MAS, P.O. Box 94079, 1090 GB Amsterdam, The Netherlands

Received 30 November 1998 and Received in final form 18 December 1998

Abstract. We study the diffusive motion of a (non-selfinteracting) chain through a quenched random environment, constructed such that it influences only the local dynamics but not the equilibrium configuration of the chain. Our Monte Carlo results show that this type of disorder, which we call kinematic, does not ruin reptation. This is in sharp contrast to disorder including also entropic traps and it supports the view that reptation prevails in melts, where in contrast to a gel entropic trapping is absent. Our data show the characteristic features of reptation, irrespective of the dilution or randomness of the kinematic obstacles. Our Monte Carlo results are in quantitative agreement with our recent detailed analytical evaluation of the reptation model (J. Stat. Phys. **90**, 1325 (1998)). The analysis suggests that we effectively see reptation of a “blob”-chain, where the size of the blob rapidly increases with decreasing obstacle concentration.

PACS. 83.20.Fk Reptation theories – 83.20.Jp Computer simulation – 83.10.Nn Polymer dynamics

1 Introduction

The diffusion of a polymer chain in a melt or through a gel is a quite complex process, which is influenced by a variety of effects. The chain moves through an entangled or crosslinked background of other chains. It, of course, cannot cross the strands of these chains, and the network of entanglements or crosslinks also does not allow the chain to locally circumvent the obstacles, like it could do with point-like objects in three dimensions. The instantaneous configuration of the chain together with the topology of the network therefore defines a tube, which constrains the motion of the chain. Since the chain is highly flexible it can not move back and forth in its tube like a rigid body, but its short time motion is restricted to the diffusion of little wiggles of “spared length”, *i.e.* short excursions of the chain perpendicular to the local tube direction move randomly along the tube axis. The large scale diffusive displacement is governed by the chain ends, which can randomly retract into the tube and then extend again in some random direction, a process known as “tube renewal”. The diffusion mechanism as described here is known as “reptation” [1]. It necessarily is the basic mode of motion of a flexible chain diffusing through a network.

In applying the reptation concept to a realistic system we, of course, have to face a number of complications, due to the fact that the entanglement network is of random structure.

- i) The local mobility of the wiggles of spared length depends on the local environment.
- ii) The tube width, *i.e.* the number of configurations that can be attained locally without changing the overall configuration of the chain, also depends on the local environment, an effect correlated with i).
- iii) The global (equilibrium) configuration of the chain depends on the disorder, since the chain preferably will be found in regions of low obstacle density. This latter effect of course is present only in a quenched disordered environment like a gel. In a melt we instead should be concerned about
- iv) relaxation of the environment, an effect, which on short length scales will be present also in a gel. Besides these kinetic or entropic features we expect for quenched disorder also energetic effects.
- v) The interaction among the mobile chain and the background will induce a locally fluctuating potential energy. On top of all this we finally have to face the excluded volume problem.
- vi) The self interaction of the mobile chain may influence both its equilibrium configuration and its dynamics.

A realistic modelling of the reptational motion should include these features, but there exists no theory which seriously treats all of these complications. The pure reptation model [1,2] neglects all the features mentioned above and treats the motion of a non-selfinteracting chain in a homogeneous tube. This is equivalent to assuming the background chains to build up the edges of a regular

^a e-mail: Isphy@next5.Theo-Phys.Uni-Essen.De

lattice. It can be argued that the self-repulsion of the chain only changes the random embedding of the tube into its environment and therefore can be included without problems. Some attempts exist to include disorder effects, especially in the long time regime [3, 4].

On the experimental side in particular numerous computer experiments have been carried through over the years (see, for instance [5–11]; physical experiments are reviewed in [12, 13]), but due to the complexity of the systems and the limitation of the available chain lengths it is hard to interpret the results. The path often followed in analyzing the data relies on comparing to asymptotic results of the pure reptation model. Typically these asymptotic results are not truly born out, and the question whether this is due to some of the complications mentioned above or just implies that the chains considered are too short for the application of asymptotic results, remains unsolved.

To illustrate this point we consider the center of mass motion of the chain:

$$g_{\text{cm}}(N, t) = \overline{\langle (\mathbf{R}_{\text{cm}}(t) - \mathbf{R}_{\text{cm}}(0))^2 \rangle}. \quad (1.1)$$

Here the pointed brackets stand for the equilibrium average over all initial chain configurations, as well as for the average over the quenched disordered environment. The bar denotes the average over all possible histories of the diffusion process. For long chains, pure reptation theory predicts this function to show two regimes:

$$g_{\text{cm}}(N, t) \sim \begin{cases} t^{1/2}/N, & T_0 \ll t \ll T_2 \\ t^\beta/N^2, & T_2 \ll t. \end{cases} \quad (1.2)$$

Here N is the chain length, T_0 denotes some microscopic time, and $T_2 \sim N^2$ is the internal equilibration time of the chain. The last line in equation (1.2) implies the reptation result for the diffusion coefficient: $D \sim N^{-2}$. These results strictly are valid for $N \rightarrow \infty$. For medium sized chains, $N \sim 100$, however, simulations even of the pure reptation model indicate some different effective behavior [7, 14]. In particular, data in the intermediate time regime $T_0 \ll t \ll T_2$ can be described by an effective power law $g_{\text{cm}} \sim t^\beta$, $\beta \sim 0.6 - 0.8$, and the diffusion coefficient decreases with a somewhat larger power of N . Now, quite similar effective laws result from a completely different model, where we ignore all topological constraints and treat the motion of an excluded volume chain in a quenched random potential [15]. Observing such behavior of g_{cm} in some complicated system showing (some) features from the list i-vi, we therefore need additional information to identify the dominant mechanism.

To improve the situation we recently in some detail have evaluated the pure reptation model also for shorter chains [16]. The results will be recalled in Section 2. They provide us with a firm basis to study the influence of disorder on the reptational motion of the chain. To proceed further and clearly separate the different effects i-vi discussed above we here analyze a model where the disorder in the environment changes only the local mobility and the local tube width, but does not introduce global entropic or

energetic traps. This is achieved by placing the polymer on a cubic lattice and the obstacles on the dual lattice. The distribution of obstacles we draw from a percolation model, where we study the whole range of obstacle densities $1 - q$ from a dense ordered obstacle lattice ($q = 0$) to unconstrained Rouse type motion ($q = 1$), *i.e.*, below and above the percolation threshold of the obstacles. In our model the equilibrium conformation of the chain stays unchanged, and we are concerned only with the kinematic effects of disorder, *i.e.*, with points i) and ii) of our list. We have carried through extensive simulations, which reveal that such purely kinematic disorder does not ruin the reptational behavior. For sufficiently long chains we find all the qualitative features characteristic of reptation. With increasing dilution of the obstacles the chain length necessary for reptational motion increases. In particular it increases quite rapidly in the range where the obstacle network ceases to percolate. We do not see any indication of an anomalous suppression of the diffusion coefficient, as found in the presence of entropic or energetic traps [6, 10], (points iii and v from our list). Indeed, all our results closely resemble those in a regular network of obstacles, but with a larger mesh size.

We are able to fit the data to our previous analytical results [16], established for a regular obstacle network of mesh size equal to the segment size of the polymer chain. We only have to adjust the chain length N_t used in the theory: $N_t = N/n_B$, where $n_B \geq 1$ increases with increasing dilution of the obstacles. The theory thus should be interpreted as describing reptative motion of a “blob” chain, where the blob size n_B depends only on the average density of the obstacles. Of course the internal dynamics of the blobs induces short time effects of motion “perpendicular to the tube”, which are not covered by reptation theory.

Our results support the general belief that chains do reptate in a melt. The only effect which might be important in a melt and which is not included here, is the relaxation of the environment, (point iv from our list). This will lead to some time dependence of the local mobility, as well as to slow local displacements of the tube (“constraint release”). Now in general quenched disorder is found to be more relevant than annealed (time dependent) disorder, and since we found no qualitative effects of quenched kinematic disorder it seems unlikely that the annealed disorder existing in a melt will qualitatively change the results. We note that the coarse graining of the chain leading to the blob picture is well known in the analysis of data for melts. In this context the blob chain often is called “primitive chain”, and n_B is known as “entanglement length”.

This paper is organized as follows. In Section 2 we briefly recall our previous analytical and numerical results [16, 14] for reptation in a narrow tube formed by regularly spaced obstacles. In the following sections we present our new results in detail. In Section 3 we define the Monte Carlo model, and we discuss the data on the qualitative level. The quantitative analysis is carried through in Section 4 and Section 5 summarizes our conclusions.

The appendix collects relevant more complicated analytical expressions derived in [16].

2 Summary of reptation results through ordered obstacle lattices

We previously analyzed the reptative motion of a non-selfinteracting chain in a dense ordered network of obstacles. Specifically we calculated the motion of the j th segment in a chain of length N :

$$g_1(j, N, t) = \overline{\langle (\mathbf{r}_j(t) - \mathbf{r}_j(0))^2 \rangle}. \quad (2.1)$$

In the long chain limit reptation theory predicts [1]

$$g_1(j, N, t) \sim \begin{cases} t^{1/4}, & T_0 \ll t \ll T_2, \\ (t/N)^{1/2}, & T_2 \ll t \ll T_3, \\ t/N^2, & T_3 \ll t, \end{cases} \quad N \gg 1 \quad (2.2)$$

where the reptation time $T_3 \sim N^3$ is the time needed for the complete destruction of the original tube. For large, but finite N , our recent analytical results [16] show rich crossover behavior among these limiting laws and furthermore show that it needs very long chains to exhibit the limiting behavior (2.2). In particular the $t^{1/2}$ -law, predicted to hold for $T_2 \ll t \ll T_3$, seems to be valid only far beyond the chain lengths which can be reached in present day computer experiments. (In physical experiments it, of course, is most difficult to measure the motion of individual segments.) Our results are rigorous as long as tube renewal can be neglected, but tube renewal can be taken into account in a seemingly quite good approximation. The analytical results, recalled in the appendix, compare very well to our simulations.

We also searched for signatures of reptation which are more significant than effective power laws. In comparison to the free diffusion of a Rouse chain in the absence of obstacles we identified two features of interest. First consider the ratio

$$\mathcal{R}_{e/m}(N, t) = \frac{g_1(0, N, t)}{g_1(\frac{N}{2}, N, t)}, \quad (2.3)$$

which measures the motion of the end segment relative to that of the central segment. For the free diffusion of a Rouse chain, this ratio takes a value of $\mathcal{R}_{e/m} = 2$ for times $t \lesssim T_2$, where $T_2 = O(N^2)$ now plays the role of the Rouse time. For reptational motion in a dense ordered obstacle lattice $\mathcal{R}_{e/m}$ initially increases to reach a maximum at $t \approx T_2$. The height of the maximum depends on the chain length, and according to our approximate theory for $N \rightarrow \infty$ it takes a limiting value $4\sqrt{2} \approx 5.66$. This strong enhancement of $\mathcal{R}_{e/m}$ should be characteristic for reptation. It quantifies the greater mobility of the end segment, which for all times $t \geq T_0$ explores the tube renewal, as compared to a central segment, which for times $t \lesssim T_3$ is confined to the initial tube. In the limit of large times,

$t \rightarrow \infty$, where the chain is displaced as a whole, $\mathcal{R}_{e/m}$ for any model reduces 1, of course.

Another qualitative signature of reptation concerns the motion of the central segment relative to the center of mass:

$$g_2\left(\frac{N}{2}, N, t\right) = \overline{\langle [\mathbf{r}_{N/2}(t) - \mathbf{R}_{cm}(t) - (\mathbf{r}_{N/2}(0) - \mathbf{R}_{cm}(0))]^2 \rangle}. \quad (2.4)$$

For large times this quantity for a noninteracting chain saturates at $g_2(\frac{N}{2}, N, t \rightarrow \infty) = R_g^2$, where R_g is the radius of gyration of the chain. For smaller times it closely follows $g_1(\frac{N}{2}, N, t)$. For a free Rouse chain, g_2 after an initial increase $g_2 \sim t^{1/2}$ at times $t \approx T_2$ smoothly bends over to saturation. For a reptating chain it will experience the two first regimes of equation (2.2). Plotting $g_2/t^{1/4}$ we, for reptation, thus expect to see an initial plateau, followed by an increase for $t \gtrsim T_2$, which for $t \approx T_3$ crosses over to a decay $g_2/t^{1/4} \sim R_g^2/t^{1/4}$. In contrast to $g_1/t^{1/4}$ the intermediate increase here is not mixed up with crossover behavior to free diffusion. It therefore is a clear signature of reptation, even if the intermediate asymptotic power law $g_2/t^{1/4} \sim t^{1/4}, T_2 \ll t \ll T_3$, is not reached.

We finally note that in our previous work we found it useful to consider besides $g_1(j, N, t)$ also the cubic invariant

$$\hat{g}_1(j, N, t) = \overline{\left\langle \sum_{\alpha=1}^3 (r_{j,\alpha}(t) - r_{j,\alpha}(0))^4 \right\rangle}^{1/2}, \quad (2.5)$$

which at least for a very narrow tube suffers much less from initial effects. Again the analytical expression is given in the appendix.

3 Monte-Carlo results

3.1 The model

We start from a model first employed by Evans and Edwards [17]. The mobile polymer chain is represented by a random walk of $N^{(MC)} - 1$ steps (“segments”) on a cubic lattice of lattice constant $\ell_0 = 1$ and lattice vectors $\mathbf{e}_\alpha, \alpha = 1, 2, 3, \mathbf{e}_\alpha \cdot \mathbf{e}_\beta = \delta_{\alpha\beta}$. The instantaneous configuration of the chain then is fixed by the set of $N^{(MC)}$ bead positions $\{\mathbf{r}_1, \dots, \mathbf{r}_{N^{(MC)}}\}$, and $\mathbf{s}_j = \mathbf{r}_{j+1} - \mathbf{r}_j, |s_j| = \ell_0 = 1$, is the vector of the j th segment. The ordered network of obstacles forms a second cubic lattice, of lattice constant $\ell_1 = m\ell_0, m = 1, 2, \dots$, placed such that the lattice points coincide with centers of cells of the first lattice. Since by this construction the obstacles do not block places on the first lattice where the polymer moves, it is guaranteed that they do not affect the equilibrium configuration of the chain. In particular, erasing obstacles we do not create entropic traps.

As microscopic motion of the chain we allow moves of hairpins and of kinks. Here a hairpin is defined as two

subsequent segments of opposite direction: $\mathbf{s}_{j+1} = -\mathbf{s}_j$. In one move it can fold onto any of the six directions $\mathbf{r}_{j-1} \pm \mathbf{e}_\alpha$, $\alpha = 1, 2, 3$, with equal probability. Kinks consist of two subsequent segments orthogonal to each other. A kink jump interchanges the segment vectors: $\mathbf{s}_j = \mathbf{e}_\alpha$, $\mathbf{s}_{j+1} = \mathbf{e}_\beta \rightarrow \mathbf{s}_j = \mathbf{e}_\beta$, $\mathbf{s}_{j+1} = \mathbf{e}_\alpha$.

The obstacles do not hinder hairpin moves, while kink jumps are allowed only if no obstacle crosses the square edged by the old and new segment vectors. We finally note that endsegments can move freely.

As is well known, in the absence of obstacles hairpin moves and kink jumps together yield Rouse dynamics. With an obstacle lattice of smallest lattice constant, $\ell_1 = \ell_0 = 1$, we suppress all kink jumps. The resulting pure hairpin dynamics yields reptation. This is the model we have analyzed in our previous work [14]. Here we start from this model ($\ell_1 = 1$), and we randomly erase a fraction q of the edges of the obstacle lattice. As stressed above, this does not affect the equilibrium configuration of the chain, but it does change the dynamics, locally allowing for kink jumps. The local mobility becomes a quenched random variable. Our computer experiments cover all the range from $q = 0$ (ordered dense lattice of obstacles, pure reptation) to $q = 1$ (no obstacles, Rouse dynamics). The obstacle lattice percolates for $q \lesssim 0.75$, and near the percolation threshold we find strong and rapid variations, but no proper transition in the qualitative behavior.

Noting from our previous work that chains of length $N^{(\text{MC})} = 160$ for $q = 0$ very clearly show reptational behavior, we in our experiments systematically varied q for this chain length. For values $q = 0.6, 0.74, 0.77$ close to the percolation threshold we also carried through experiments for longer chains, going up to $N^{(\text{MC})} = 1280$ for $q = 0.77$. An individual run extends to 10^8 Monte Carlo steps, and we took a moving time average, extracting data up to $t^{(\text{MC})} = 10^7$ MC steps. We generally averaged over forty runs, each in a different realization of the disorder, but some experiments at high dilution ($q \geq 0.74$) are taken with lower statistics. As we will see, in that range our analytical theory cannot reasonably be applied for the chain lengths considered, since the time window, where reptation dominates, becomes too small. We therefore here are content with less precise data, showing the qualitative trends. The mean square deviation of the data used in the quantitative analysis is less than 5% for $t^{(\text{MC})} = 10^7$, and it rapidly decreases with decreasing time. Typical error bars are given in the plots.

To see the influence of the tube width and to compare to our results in a disordered environment we also carried through experiments with an ordered obstacle lattice of lattice constant $\ell_1 = 2$, *i.e.* with every second row of obstacles removed in all three spatial directions.

3.2 Center-of-mass motion

In Figure 1 we show some of our results for the center-of-mass motion, where we divided out the expected intermediate asymptotics $g_{\text{cm}}(t) \sim t^{1/2}/N$. Figure 1a shows the results for $N^{(\text{MC})} = 160$ and degrees of dilution q covering

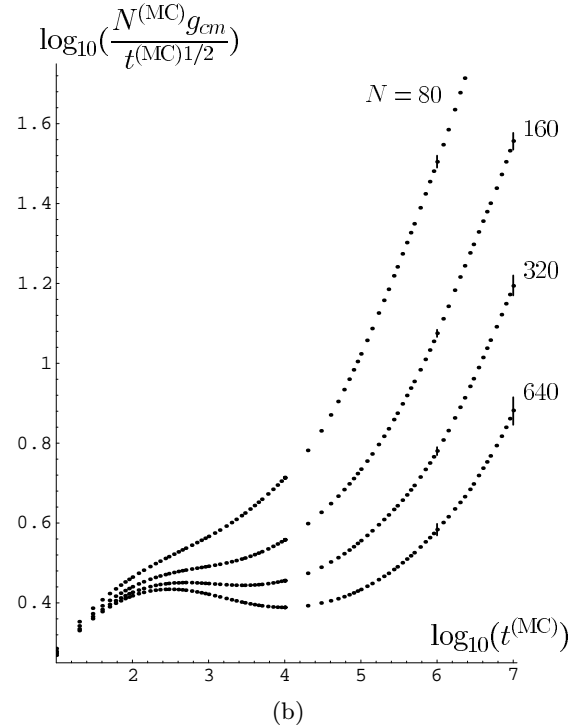
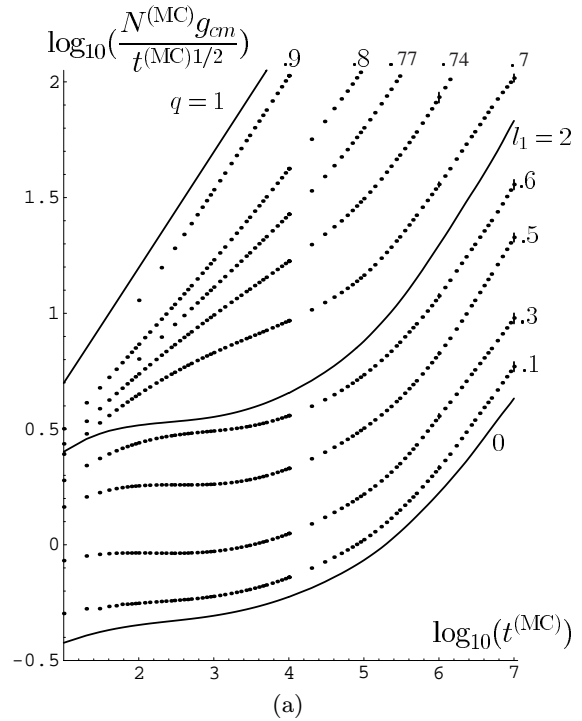


Fig. 1. $\log_{10}(N^{(\text{MC})} g_{\text{cm}}(N, t)/(t^{(\text{MC})})^{1/2})$ as function of $\log_{10} t^{(\text{MC})}$. (a) Simulation data for $N^{(\text{MC})} = 160$. Values of q as given. The full lines represent the data for ordered systems $\ell_1 = 1$ (*i.e.* $q = 0$), $\ell_1 = 2$, or $q = 1$ (*i.e.* Rouse). Error bars, showing the mean squared deviation, are given for $\log_{10} t^{(\text{MC})} = 7$ and 6, the latter being almost invisible. (b) Data for $q = 0.6$ and $N^{(\text{MC})} = 80, 160, 320, 640$. Error bars as in (a).

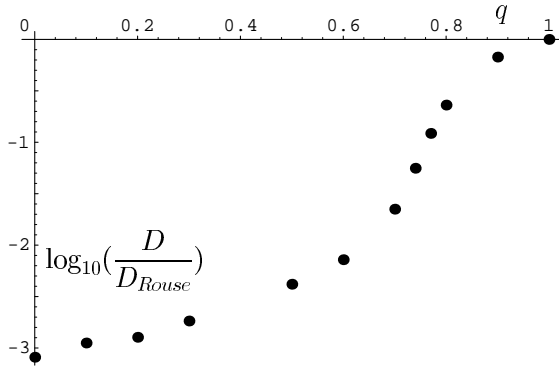


Fig. 2. $\log_{10} D/D_{\text{Rouse}}$ as function of q for $N^{(\text{MC})} = 160$.

the whole range $0 < q < 1$. We also included the results found for ordered obstacle lattices $\ell_1 = 1, 2$ and the result for the free Rouse chain ($q = 1$). As a first observation we note that up to dilution $q = 0.6$ the results closely resemble those in an ordered lattice of obstacles. Indeed the curve for the ordered obstacle lattice $\ell_1 = 2$ nicely falls among the others. The results somewhat change their character in the fairly small interval $0.7 \leq q \leq 0.77$, comprising the percolation threshold. For larger q -values we see Rouse-type behavior, weakly modified by the disorder.

Searching for power law behavior, we easily can find parameter ranges where the data over one to two decades follow a law $g_{\text{cm}} \sim t^\beta$, for almost any β in the interval $1/2 \lesssim \beta \lesssim 1$. In the range $0.3 \lesssim q \lesssim 0.6$ there even seems to hold the expected intermediate law $g_{\text{cm}} \sim t^{1/2}$. This at first is somewhat surprising, since such behavior for $N^{(\text{MC})} = 160$ is not found in the ordered lattice $\ell_1 = 1$, and we know from Figure 12 of [14] that even with such a dense regular obstacle lattice it needs longer chains to observe that law. Indeed we here are misled by initial effects. This is clearly shown in Figure 1b, where we plot data for $q = 0.6$ and several chain lengths. The $t^{1/2}$ -plateau seen for $N^{(\text{MC})} = 320$ is a transient feature, not stable against increasing chain length. We expect the proper plateau for $q = 0.6$ to develop only for $N^{(\text{MC})} \gtrsim 640$.

For $N^{(\text{MC})} \leq 160$ we can estimate the diffusion coefficient from the large-time behavior of g_{cm} . Figure 2 shows our results for $N^{(\text{MC})} = 160$ as function of q . We see some rapid variation near the percolation threshold (note the logarithmic scale of D/D_{Rouse} !), but a purely monotonic behavior for all values of q , *i.e.* no sign of dropping below the reptation limit. This is in contrast to results found for disorder inducing entropic or energetic traps [10].

3.3 Motion of the central segment

In our previous work we found that the intermediate $t^{1/4}$ -regime for the motion of the central segment shows up most clearly in the cubic invariant \hat{g}_1 (Eq. (2.5)). The initial behavior of the second moment g_1 (Eq. (2.1)) suffers from a slow transient that reflects the discreteness of the

basic stochastic process. The same feature is found here, and we therefore in Figure 3 show results for \hat{g}_1 . Our data for $N^{(\text{MC})} = 160$ are given in Figure 3a. We observe the same trend as found for the center-of-mass in Figure 1a. Reptation like behavior persists up to $q = 0.7$, and transforms into weakly modified Rouse type behavior in the interval $0.7 \lesssim q \lesssim 0.8$. The data for the ordered obstacle lattice $\ell_1 = 2$ nicely fall between the curves $q = 0.6, 0.7$. For $q \leq 0.6$ the $t^{1/4}$ -plateau is clearly developed, with small, but visible, initial effects, which for $q = 0.5, 0.6$, or $\ell_1 = 2$ produce a shallow maximum. As is illustrated by the lower set of curves in Figure 3b, we here indeed observe the intermediate asymptotics, even for $q = 0.6$.

The data shown in Figures 1a, 3a might lead to the suspicion that reptation generally breaks down near the percolation threshold. We believe this to be not the case, and a first hint is given by the data of Figure 3b, where we show $\hat{g}_1/t^{(\text{MC})1/4}$ for $q = 0.6, 0.74, 0.77$ and increasing chain lengths. With increasing q we clearly see a strong increase of the initial effects, so that the range of $t^{1/4}$ -behavior only begins for larger t . But we also see that for q fixed the data with increasing $N^{(\text{MC})}$ bend over towards reptational behavior. The data for $q = 0.74, N^{(\text{MC})} = 640$, show a small plateau, quite similar to that found for $q = 0.6, N^{(\text{MC})} = 80$. The data $q = 0.77, N^{(\text{MC})} = 1280$, resemble those for $q = 0.74, N^{(\text{MC})} = 160$ or 320. This suggests that reptation survives also beyond the percolation threshold of the obstacle lattice, but that the chain length necessary to observe it, increases dramatically.

According to our previous findings a clear signature of reptation can be found by measuring $g_2(\frac{N}{2}, N, t)$, which gives the motion of the central segment relative to the center-of-mass. In the interval $T_2 \lesssim t \lesssim T_3$ reptation leads to an increase of $g_2/t^{1/4}$. This increase is due to spared length diffusing in from the chain ends, and it is cut off by the tube renewal. Figure 4a shows data for $N = 160$. For $q \leq 0.6$ and also for $\ell_1 = 2$ the expected maximum is clearly seen, and the reptation mechanism must be valid. With increasing q the maximum, however, becomes less and less pronounced, and for $q \geq 0.7$ the structure of a plateau followed by a maximum is lost, indicating that the interval $T_2 \lesssim t \lesssim T_3$ becomes too short. As expected the maximum becomes stronger with increasing chain length, as illustrated in Figure 4b for $q = 0.6$. We note that even in the initial range the data for different chain lengths do not fall on top of each other. Comparing to Figures 1b, 3b, we see that this reflects initial effects in the behavior of the center of mass.

Analyzing the data for $q = 0.77$ we do not find a structure similar to Figure 4b even for $N^{(\text{MC})} = 1280$. In view of Figure 3b this is not too surprising, since, as shown there, the time window where reptation might dominate, shrinks rapidly.

3.4 Motion of the end segment

As we have found previously, the motion of the end segment shows very large initial effects, which are due to two different sources. First, the end segment in a single

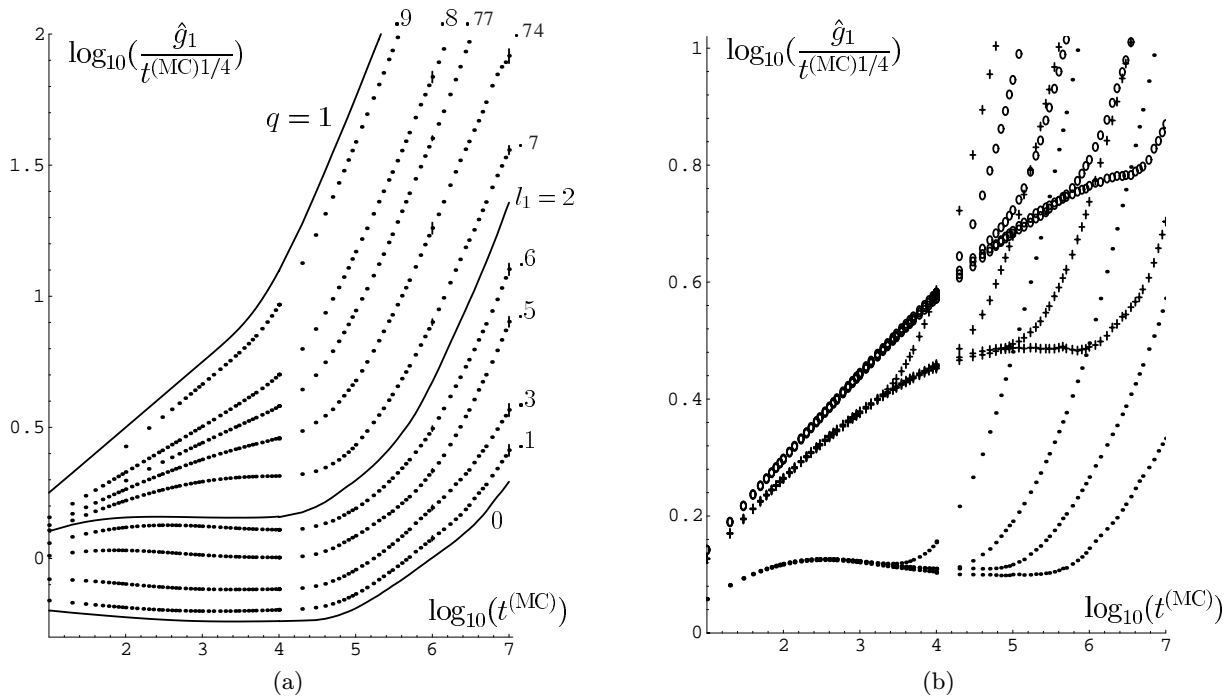


Fig. 3. $\log_{10} \left(\hat{g}_1 \left(\frac{N}{2}, N, t \right) / (t^{(\text{MC})})^{1/4} \right)$ as function of $\log_{10} t^{(\text{MC})}$. (a) Data for $N^{(\text{MC})} = 160$, plot corresponding to Figure 1a. (b) Data for $q = 0.6$, $N^{(\text{MC})} = 80, 160, 320, 640$ (from the left), shown as points; $q = 0.74$, $N^{(\text{MC})} = 80, 160, 320, 640$ (crosses); $q = 0.77$, $N^{(\text{MC})} = 160, 320, 640, 1280$ (circles).

Monte Carlo step jumps a mean square distance $c_1 = 2\ell_0^2 = 2$, an effect not taken into account in the reptation model. (The corresponding correction for an interior segment is much smaller: $c_0 = 2/9$.) The second and less trivial effect is inherent in the reptation model. To calculate $g_1(0, N, t)$ we have to determine the maximal retraction into the tube of chain end $j = 0$ within the time interval t . This is a complicated problem which analytically we could solve only approximately. We found that the correlations inherent in the reptational process together with the discreteness of the elementary motion yield a result which only very slowly and for very long chains develops the expected intermediate $t^{1/4}$ behavior. This finding is in agreement with our Monte Carlo results for the dense regular obstacle lattice $\ell_1 = 1$. The same effects clearly are present here. We therefore do not show our results for $g_1(0, N, t)/t^{1/4}$, and only note that a plot of the data for $N^{(\text{MC})} = 160$ closely resembles Figures 1a, 3a. For $q \leq 0.6$ the results are similar to those for ordered obstacle lattices, and they approach Rouse-type behavior for $q \gtrsim 0.8$. The curve for $\ell_1 = 2$ falls in between the data with dilutions $q = 0.6, q = 0.7$.

The behavior of the ratio $\mathcal{R}_{e/m} = g_1(0, N, t) / g_1 \left(\frac{N}{2}, N, t \right)$ is of more interest. As recalled in Section 2, a clear increase of this ratio above the Rouse value $\mathcal{R}_{e/m} = 2$ is one signature of reptation. Furthermore the maximum of $\mathcal{R}_{e/m}$ should be attained for $t \lesssim T_2$, a time range that is easily reached in simulations. A significant test of this prediction therefore is much easier than the observation of the structure in $g_2 \left(\frac{N}{2}, N, t \right) / t^{1/4}$, expected for larger

times $T_2 \lesssim t \lesssim T_3$. Figure 5 shows our results for $\mathcal{R}_{e/m}$ for dilutions $q = 0.6$ and $q = 0.77$. For $q = 0.6$ we find pronounced maxima, the height increasing with increasing $N^{(\text{MC})}$. The set of curves is quite similar to the results found for the regular obstacle lattice, $\ell_1 = 1$, (see [14], Fig. 9). Again we conclude that the chains clearly exhibit reptational motion. We, however, here observe a quite similar trend for $q = 0.77$, *i.e.*, above the percolation threshold. Except of the slope of the initial increase there is no significant difference compared to the data for $q = 0.6$ and maximal values $\mathcal{R}_{e/m}^{[\text{max}]} \approx 3$ are reached. This suggests that also above the percolation threshold, reptation will be the dominant mode of motion beyond some short time regime, provided the chains are long enough. The “short time” regime, however, may be very large.

Figure 6 supports that view. We there have plotted the measured maxima of $\mathcal{R}_{e/m}$ against the dilution q . For $N^{(\text{MC})} = 160$ we see a steep decrease for $0.6 \leq q \leq 0.8$, but the increase of the maxima with increasing chain length $N^{(\text{MC})}$ for $q = 0.77$ is quite similar to that found for smaller q .

3.5 Discussion

Our results show that medium sized chains do reptate in a percolating irregular network of obstacles, which modifies the local kinetics only, and does not change the equilibrium configuration. Indeed, for $q \lesssim 0.6$ the results in

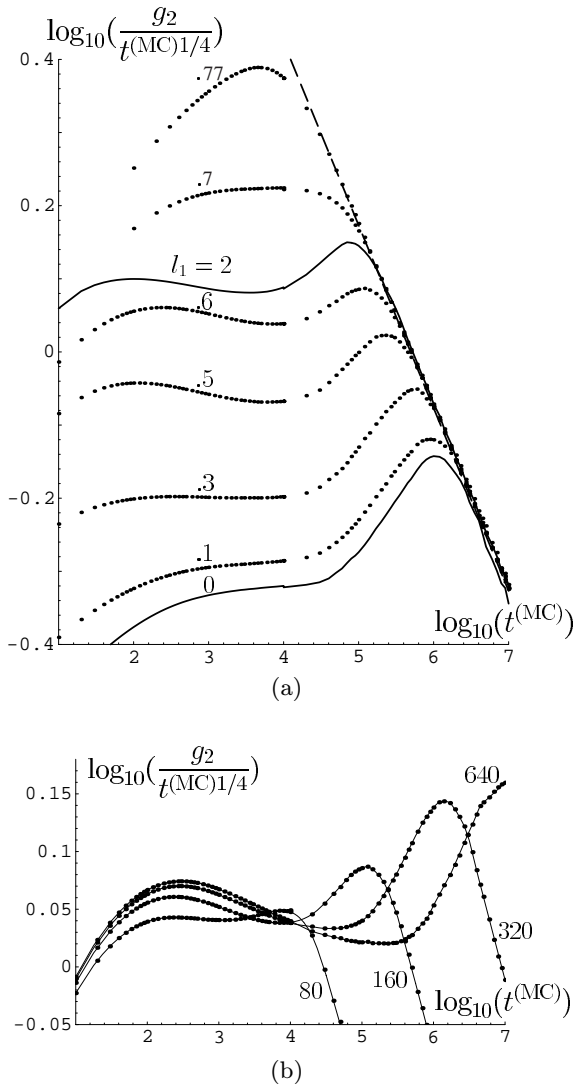


Fig. 4. $\log_{10} \left(g_2 \left(\frac{N}{2}, N, t \right) / (t^{(\text{MC})})^{1/4} \right)$ as function of $\log_{10} t^{(\text{MC})}$. (a) Data for $N^{(\text{MC})} = 160$ and q -values as given. The curves represent data in the ordered lattices $\ell_1 = 1$ and $\ell_1 = 2$. The broken line corresponds to saturation: $R_g^2 / (t^{(\text{MC})})^{1/4}$. (b) Data for $q = 0.6$, $N^{(\text{MC})} = 80, 160, 320, 640$ (from the left). Lines serve to guide the eye.

all respects are most similar to reptation in an ordered network. This suggests that the effect of disorder in that range of q can be modelled by considering the motion of a chain through an effective ordered network of properly adjusted bond length. This amounts to adjusting the width of the effective tube, or the blob size, equivalently. We will pursue this idea in the next section.

Above the percolation threshold the characteristic features of reptation rapidly are lost for shorter chains, but we have evidence that with increasing chain length we again enter the reptational regime. This implies that the main effect of passing over the percolation threshold is a rapid decrease of the effective number of entanglements.

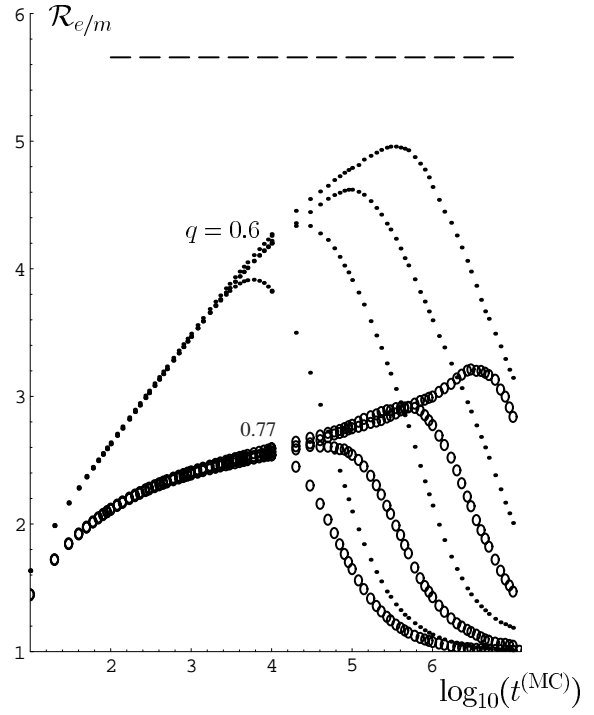


Fig. 5. $\mathcal{R}_{e/m}$ (Eq. (2.3)) as function of $\log_{10} t^{(\text{MC})}$. The data are corrected for initial effects by subtracting $c_1 = 2$ or $c_0 = 2/9$ from the endpoint or the mid-point motion. Data: $q = 0.6$, $N^{(\text{MC})} = 80, 160, 320, 640$ (points, from the left). $q = 0.77$, $N^{(\text{MC})} = 160, 320, 640, 1280$ (circles). The broken line gives the theoretical value $4 \cdot 2^{1/2}$ for the maximum in the long chain limit.

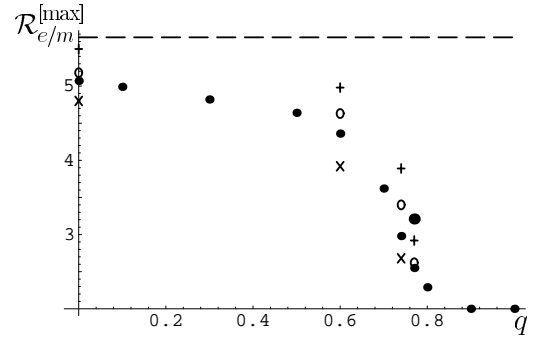


Fig. 6. Maxima of $\mathcal{R}_{e/m}$ as function of q . Symbols: (\times) $N^{(\text{MC})} = 80$; (\bullet) $N^{(\text{MC})} = 160$; (\circ) $N^{(\text{MC})} = 320$; ($+$) $N^{(\text{MC})} = 640$; (\bullet) $N^{(\text{MC})} = 1280$. The reptation prediction for $N \rightarrow \infty$ is the dotted line. The Rouse value $\mathcal{R}_{e/m}^{[\text{max}]} = 2$ coincides with the q -axis.

However, the density of entanglements does not vanish for any $q < 1$. A naive estimate is given by the probability to find four occupied bonds of the obstacle lattice ($\ell_1 = 1$), forming a square. The probability to find such a “slip link” surrounding a given bond of the lattice, where the polymer moves, equals $(1 - q)^4$. Thus on the average a polymer of length N will pass through $(1 - q)^4 N$ slip links, and stability of reptational motion also in very dilute

systems amounts to the statement that a finite number of slip links on the chain is sufficient to enforce reptation on large time scales. Calculating $(1 - q)^4 N^{(\text{MC})}$ for $q = 0.77$, $N^{(\text{MC})} = 1280$, or $q = 0.74$, $N^{(\text{MC})} = 640$, we find values of 3.6 or 2.9, respectively. This clearly is only a lower bound for the number of entanglements, and the analysis of the next section suggests that the effective number of entanglements may be larger, but not dramatically so.

4 Quantitative comparison to reptation theory

4.1 Parameters

In previous work [14] we have found that the data for the dense ordered obstacle lattice $\ell_0 = 1$ are consistent with the results of an analytical evaluation [16] of the reptation model. The agreement is excellent for the motion of the central segment in the time range $t \ll T_3$, where tube renewal is negligible. For larger times $t \approx T_3$ or for the motion of the end segment in all the regime $t < T_3$, tube renewal is important. We suggested a ‘‘mean hopping rate’’ approximation, which ignores correlations, and which accounts quite well for tube renewal corrections on the motion of the inner segments. It somewhat underestimates the motion of the end segment. In the appendix we recollect those of our analytical results needed here.

The theory models the wiggles of spared length as non-interacting particles, which randomly hop along the chain. The model involves some parameters, which can well be estimated by order of magnitude, but which cannot be fixed precisely *a priori*. These are the hopping probability p and the equilibrium density ρ_0 of the particles on the chain, as well as the spared length ℓ_s per particle. We also should note the segment size ℓ_B of the chain, which did not show up explicitly in our previous work, since the dense regular obstacle lattice and the lattice on which the polymer moves were taken to have the same lattice constant: $\ell_1 = \ell_0 = 1$. Then clearly ℓ_B is to be identified with ℓ_0 , but for more diluted obstacle configurations such identification is not obvious. Below we will find that both in the ordered lattice $\ell_1 = 2$ and in the disordered obstacle lattices the theory describes the motion of an effective blob chain, with $\ell_B > \ell_0$. We note that both ℓ_s and ρ_0 are defined with respect to ℓ_B . In particular, the dimensionless parameter ℓ_s is the spared length per particle, measured in fractions of the segment size ℓ_B .

It turns out that the choice of the hopping probability p is fairly irrelevant, provided we express our results in terms of $\hat{t} = pt$. It weakly influences the results for $\hat{t} \lesssim 1$, only. We therefore follow [14] in setting $p = 1/5$, and we do not consider this parameter any more. We thus are left with three the model parameters ℓ_B , ℓ_s , and ρ_0 . The most relevant parameter of the model is the combination $\ell_B^2 (\ell_s^2 \rho_0)^{1/2}$, which determines the motion of the central segment for $T_0 \ll t \ll T_3$. Tube renewal effects and the ratio $\mathcal{R}_{e/m}$ are sensitive to ℓ_B^2 (or $\ell_s^2 \rho_0$) separately, which thus makes for a second important parameter. Finally, ρ_0

influences the size of the initial effects found in g_1 , but not in \hat{g}_1 . For long chains, where $T_0 \ll T_2$, it is only of secondary importance.

In comparing to the simulation data we first have to relate the Monte Carlo chain length $N^{(\text{MC})}$ to the theoretical chain length $N = N_t$. Previously (see [14], Sect. II.C) we used $N_t = N^{(\text{MC})} - 3$, where the correction takes into account that $N^{(\text{MC})}$ counts the beads whereas N_t counts the segments, and that the theory does not account for the rapid jumps of the end segments. In the present work we must be prepared for the theory to describe a coarse grained chain of effective segment size ℓ_B , and we determine N_t by equating the end-to-end distances of the Monte Carlo chain and the theoretical chain. We thus find

$$N_t = \left(N^{(\text{MC})} - 3 \right) / \ell_B^2, \quad (4.1)$$

and we identify the number of elementary segments (of size $\ell_0 = 1$) per blob as $n_B = \ell_B^2$. Furthermore we have to introduce a time scale τ that relates \hat{t} to the Monte Carlo time $t^{(\text{MC})}$:

$$\hat{t} = \tau t^{(\text{MC})}. \quad (4.2)$$

Finally the motion of the Monte Carlo chain will be affected by the larger tube width. We therefore should subtract a (constant) contribution due to motion perpendicular to the tube axes. We thus for the central segment write

$$g_1 \left(\frac{N_t}{2}, N_t, \hat{t} \right) = g_1^{(\text{MC})} \left(\frac{N^{(\text{MC})}}{2}, N^{(\text{MC})}, t^{(\text{MC})} \right) - b_1$$

$$\hat{g}_1 \left(\frac{N_t}{2}, N_t, \hat{t} \right) = \left[\left(\hat{g}_1^{(\text{MC})} \left(\frac{N^{(\text{MC})}}{2}, N^{(\text{MC})}, t^{(\text{MC})} \right) \right)^2 - b_2^2 \right]^{1/2}. \quad (4.3)$$

In the ordered obstacle lattice $\ell_1 = 1$ the parameter b_1 coincides with $c_0 = 2/9$ (see [14], Eq. (2.10)). Previously we found that the effects of c_0 and of ρ_0 are most similar, so that a change of one of these parameters can be compensated by changing the other. The same observation holds here, and we can therefore set one of these parameters to some reasonable value from the outset. In the sequel we choose

$$b_1 = \frac{\ell_B^2}{6}. \quad (4.4)$$

This is motivated by noting that the segment size ℓ_B of the theoretical chain will play the role of the end-to-end distance of an effective blob of the Monte Carlo chain. The average transverse excursions of a specific segment will be of the order of the radius of gyration $\ell_B/\sqrt{6}$ of this blob.

Similar corrections for excursions not accounted for by the theoretical model clearly apply also for the end segment. Since, however, the theory for the end segment is

Table 1. Maximal values of $\mathcal{R}_{e/m}$ in the ordered obstacle lattices.

	$N^{(\text{MC})} - 3$	17	37	77	157	317	637
$\mathcal{R}_{e/m}^{[\text{max}]}$	$\ell_1 = 1$	4.16	4.50	4.80	5.07	5.18	5.5
	$\ell_1 = 2$	-	-	-	4.26	4.56	4.9

not on the same level of rigour as for the central segment, we do not try to introduce corresponding corrections, except that we always subtract the contribution of local jumps, $c_1 = 2$. In particular, the Monte Carlo value of the ratio $\mathcal{R}_{e/m}$ is determined by subtracting c_1 or c_0 from the motion of the end segment or the central segment, respectively.

4.2 Effects of a wider regular tube

We first analyze the data for the ordered obstacle lattice $\ell_1 = 2$. This will give us some feeling for the typical effects of the tube width on the reptational behavior.

In [16], Section IV, we have given an expression for the motion of the central segment $g_1(\frac{1}{2}N_t, N_t, t)$, which is exact for $T_0 \ll t \ll T_3$. The result depends on two rescaled variables, which in terms of the Monte Carlo variables can be expressed as

$$\ell_B^2 \hat{t}^{1/4} = \ell_B^2 (\ell_s^2 \rho_0)^{1/2} (\tau t^{(\text{MC})})^{1/4}$$

$$\frac{\hat{t}}{N_t^2} = \frac{\ell_B^4}{(N^{(\text{MC})} - 3)^2} \tau t^{(\text{MC})}, \quad (4.5)$$

(see also the appendix). Comparing theory and experiment in that time window we determine the combinations $\ell_B^2 (\ell_s^2 \rho_0)^{1/2} \tau^{1/4}$ and $\ell_B^4 \tau$ with high precision. The uncertainty is of the order of 1 % or less. Due to the scaling properties we however gain no information on ℓ_B^2 and thus on the tube width.

Such information is contained in the maximal value $\mathcal{R}_{e/m}^{[\text{max}]}$ taken by the ratio $\mathcal{R}_{e/m}$ as function of t for $t \approx T_2$. For the dense obstacle lattice $\ell_B = \ell_1 = \ell_0 = 1$ we have found that $\mathcal{R}_{e/m}^{[\text{max}]}$ depends on $N_t = N^{(\text{MC})} - 3$. Table 1 gives the previously determined values, together with the values found here for $\ell_1 = 2$. As is obvious, the chains for $\ell_1 = 2$ correspond to shorter chains embedded in the dense obstacle lattice $\ell_1 = 1$. We now determine N_t for $\ell_1 = 2$ as the value of the chain length, that yields the observed value $\mathcal{R}_{e/m}^{[\text{max}]}$ for dense obstacles, $\ell_1 = 1$. We thus map the Monte Carlo chain onto a shorter reptating blob chain. The chain length dependence of $\mathcal{R}_{e/m}^{[\text{max}]}$ is not very strong, (in fact it saturates for $N \rightarrow \infty$), and we therefore cannot determine the values of N_t with high precision. The three chain lengths used in our experiments yield values $\ell_B^2 = (N^{(\text{MC})} - 3) / N_t \approx 6.5 - 7.5$. This uncertainty, however, is quite tolerable, just because the results are not to sensitive to ℓ_B^2 (or N_t , equivalently). We choose

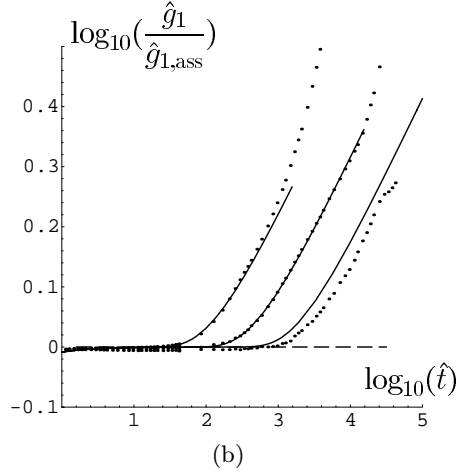
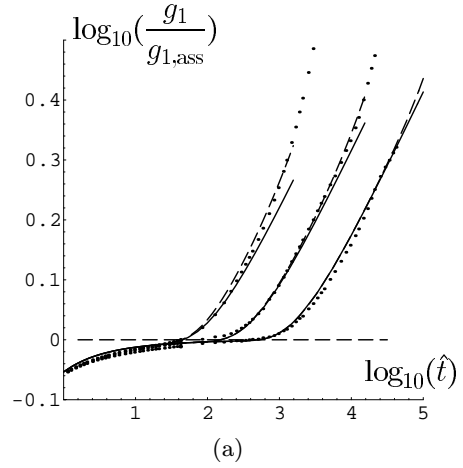


Fig. 7. Motion of the central segment for the ordered obstacle lattice $\ell_1 = 2$, as function of $\log_{10} \hat{t}$. Chain lengths $N^{(\text{MC})} = 160, 320, 640$ (from the left). Dots: Simulation data. (a) $\log_{10}(g_1(\frac{N_t}{2}, N_t, t) / g_{1,\text{ass}}(t))$, where $g_{1,\text{ass}}(t) = 2\ell_B^2 (\ell_s^2 \rho_0)^{1/2} \pi^{-3/4} \hat{t}^{1/4}$ gives the intermediate asymptotic power law, valid for $T_0 \ll t \ll T_2$. Full lines: tube renewal neglected (Eq. (A.2)); broken lines: with tube renewal (Eq. (A.1)). The horizontal broken line represents the intermediate asymptotics. (b) $\log_{10}(\hat{g}_1(\frac{N_t}{2}, N_t, t) / \hat{g}_{1,\text{ass}}(t))$, $\hat{g}_{1,\text{ass}}(t) = \sqrt{\frac{\pi}{2}} g_{1,\text{ass}}(t)$. Curves represent the theory without tube renewal (Eq. (A.9)). All analytical curves end at $T_3(N^{(\text{MC})})$, determined from the motion of the end segment: $\langle (r_0(T_3) - r_0(0))^2 \rangle = R_g^2$.

$\ell_B^2 = 7.5$, with a resulting value of $b_1 = \ell_B^2 / 6 = 1.25$. b_2 (Eq. (4.3)) should be of the same order of magnitude. Finally we determine ρ_0 by adjusting the initial behavior of $g_1(\frac{1}{2}N_t, N_t, \hat{t})$.

The resulting fits are shown in Figures 7 and 8. We used parameters

$$\ell_B^2 = 7.5, \quad \ell_s^2 \rho_0 = 0.492, \quad \tau = 4.2 \times 10^{-3},$$

$$\rho_0 = 1.4, \quad b_1 = 1.25, \quad b_2 = 1.2.$$

Figures 7a or b should be compared to Figures 6 or 7 of [14], where we should note that in the previous work we

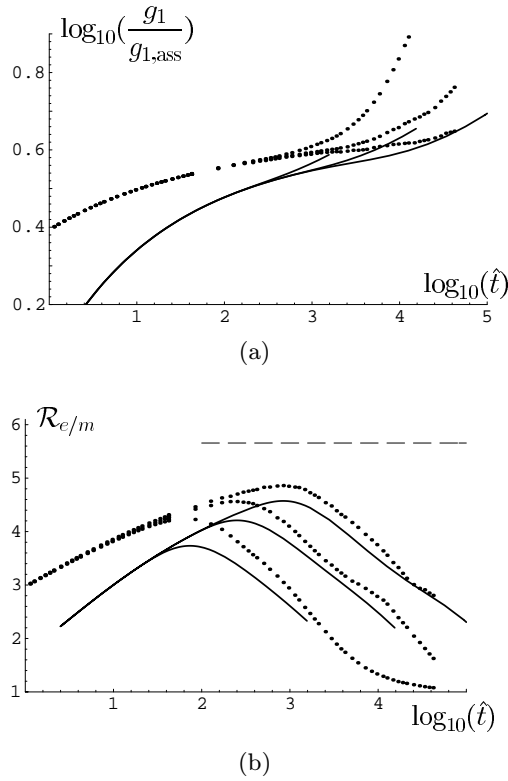


Fig. 8. Motion of the end segment for $\ell_1 = 2$ Chain lengths $N^{(\text{MC})} = 160, 320, 640$ (from the left). Theoretical curves again end at $T_3(N^{(\text{MC})})$. (a) $\log_{10}(g_1(0, N_t, \hat{t})/g_{1,\text{ass}}(\hat{t}))$, $g_{1,\text{ass}}(\hat{t}) = 2\ell_B^2(\ell_s^2\rho_0)^{1/2}\pi^{-3/4}\hat{t}^{1/4}$. Curves represent the approximation (A11). (b) $\mathcal{R}_{e/m}(\hat{t}) = g_1(0, N_t, \hat{t})/g_1(\frac{N_t}{2}, N_t, \hat{t})$. The broken line represents the theoretical asymptote. Full curves represent the theoretical approximation.

did not include a parameter b_2 to correct the initial behavior of \hat{g}_1 . Figures 8a or b are the counterparts of Figures 8 or 9 of [14]. We find no difference in the quality of the fit for $\ell_1 = 2$ as compared to $\ell_1 = 1$. The figures are almost indistinguishable. In particular, the motion of the central segment is fitted most precisely, with tube renewal corrections of the correct order of magnitude showing up in the correct time region. For the motion of the end segment the deviations among theory and data are the same as found previously for $\ell_1 = 1$. This supports the view that motion through a wider (regular) obstacle lattice can be considered as reptation of a coarse grained “blob” chain.

4.3 Environments with kinematic disorder

Inspection of the data (see Figs. 1, 3-5) suggests that at least up to dilution $q = 0.6$ the chain motion can be described as reptation in a wider tube. To put this statement on a firmer basis we quantitatively have evaluated the data, following the procedure outlined in the previous subsection. To give an example, we show in Figures 9 and 10 our results for $q = 0.6$. Clearly no significant difference

Table 2. Values of the parameters used in the theoretical analysis.

q	0.0	0.1	0.3	0.5	0.6
ℓ_B^2	1	1.36	1.94	3.27	6.34
τ	0.061	0.051	0.030	0.0115	0.0030
$\ell_s^2\rho_0$	1.23	0.844	0.808	0.806	0.671
ρ_0	0.22	0.34	0.60	1.2	2.5
b_1	2/9	0.23	0.32	0.55	1.06
b_2	—	0.4	0.6	1.0	1.9

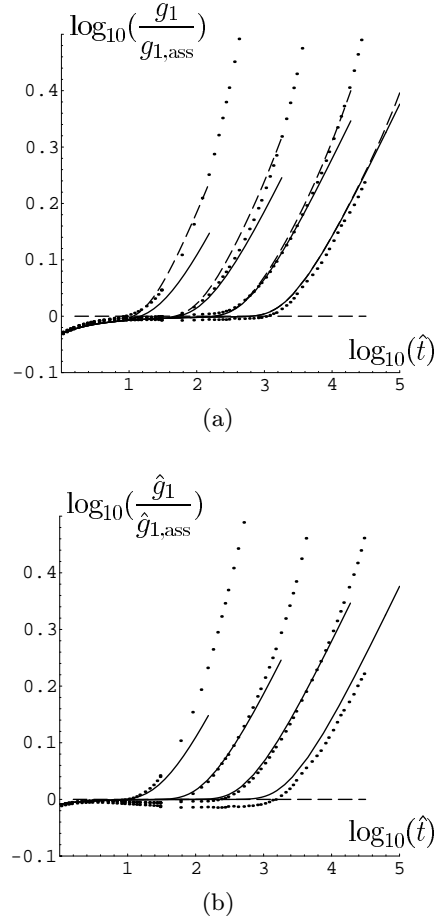


Fig. 9. Motion of the central segment for dilution $q = 0.6$, chain lengths $N^{(\text{MC})} = 80, 160, 320, 640$. Curves as in Figure 7.

compared to the results in the ordered lattice $\ell_1 = 2$ is visible. We found most similar plots for all $q < 0.6$. This shows that kinematic disorder has no qualitative influence on the motion of the chain. The concept of a blob chain reptating in an effective tube is well able to explain the data.

Clearly, in view of the number of parameters involved in the fits one might doubt whether our finding really proves the blob concept. To support our interpretation a closer look at the parameter values, as given in Table 2,

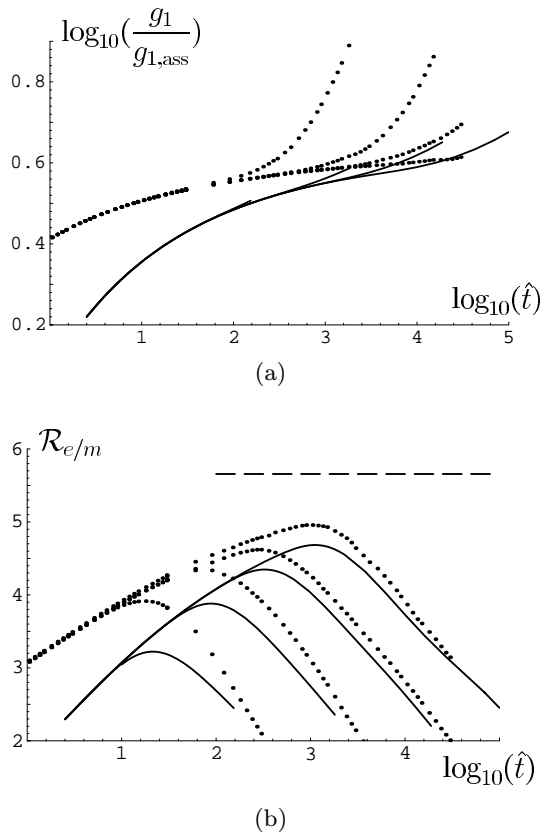


Fig. 10. Motion of the end segment for $q = 0.6$, $N^{(\text{MC})} = 80, 160, 320, 640$. As in Figure 8.

is appropriate. We first consider the blob size ℓ_B^2 , which, – as expected –, is found to increase with increasing dilution of the obstacles. The value reached for $q = 0.6$ seems quite reasonable in view of our result $\ell_B^2 = 7.5$ for $\ell_1 = 2$, *i.e.* for the ordered obstacle configuration where 3/4 of the obstacles are erased. In this latter situation we would expect $\ell_B = \ell_1 = 2$ as a lower bound, and the larger value $\ell_B = \sqrt{7.5} \approx 2.74$ just means that the chain with finite probability leaks out to neighbouring cells of the obstacle lattice. The parameter τ decreases with increasing q , which implies that with increasing blob size, it needs more Monte Carlo steps for a blob to move one step on the coarse grained chain. Indeed, $1/\tau$ roughly is proportional to the Rouse time $T_B \sim n_B^2 = \ell_B^4$ of a blob. The density ρ_0 of effective particles on the blob chain should be bounded from below by the density $\rho_0 = 0.22$ in the dense obstacle lattice, multiplied by ℓ_B^2 to account for the larger segment. Again this is well fulfilled. With increasing q , ρ_0 gradually increases relative to that bound, which can be interpreted as an increasing kink contribution to the mobility. The parameter b_1 has been fixed to $b_1 = \ell_B^2/6$, consistent with the blob picture, and $b_2 \approx 1.8b_1$ holds for all q . Such a relation seems reasonable since the fourth moment defining \hat{g}_1 puts larger weight on large transverse excursions than does the second moment (g_1). In summary, the param-

eters extracted are consistent with plausible estimates and show a variation as expected for a blob chain.

We restricted our quantitative analysis to $q \leq 0.6$, even though we believe that reptational motion will be present for all $q < 1$, if only the chains are sufficiently long. However, for the chain lengths used in our experiments with $q \geq 0.7$, the region showing signs of reptation is too small for any meaningful quantitative analysis. For instance, for $q = 0.7$, $N^{(\text{MC})} = 160$, we find from the measured value of $\mathcal{R}_{e/m}^{(\text{max})}$ a rough estimate $20 \lesssim \ell_B^2 \lesssim 30$, corresponding to a blob chain of length $8 \gtrsim N_t \gtrsim 5$. Such a chain is too short for reptational behavior to show up unambiguously. All the chains used in our experiments for $q \geq 0.7$ seem to correspond to blob chains of lengths $N_t < 10$, which for $q = 0.77$, $N^{(\text{MC})} = 1280$, in particular, implies $\ell_B^2 > 130$. We thus suggest that the effective blob size ℓ_B rapidly increases near and above the percolation threshold $q \approx 0.75$, but we also suggest that this is the only important effect of percolation of the obstacles on the chain dynamics. We note that the onset of that rapid increase of ℓ_B^2 is seen already for $q = 0.6$. (Tab. 2)

Are there theoretical arguments to support our observation that polymer dynamics is stable against kinematic disorder? Indeed, we may note two results, which in some sense complement one another. Starting from the standard Langevin equation of the Rouse model without obstacles, we may analyze the effect of quenched disorder in the local mobility. It is found [18] that such disorder is irrelevant in the renormalization group sense, which means that it does not change the power law behavior. The diffusion coefficient, for instance, still behaves as $D = a/N$. Only the proportionality constant a depends on the disorder, an effect which can be calculated perturbatively.

The second result concerns the effect of quenched disorder in the hopping probability p for a one dimensional hopping problem. Taking p to depend on the position of the step, $p \rightarrow p(j, j') \equiv p(j', j)$, $j' = j + 1$, one still finds normal diffusional behavior of the particles, as long as $p(j, j') > p_0 > 0$. The diffusion coefficient of the particles is given by some average of the hopping rates [19]. In our problem the local hopping rates are bounded from below by the mobility of the hairpins, and thus the above result almost applies to the diffusion of the spared length, except for a small difference in the problems considered. In our case the hopping rates are not fixed relative to the chain, on which the spared length diffuses, but they are fixed in the space, through which the chain slowly moves. Still we feel that both the pieces of theoretical information quoted here strongly suggest that kinematic disorder cannot qualitatively change the dynamical behavior of the chain.

We, however, in this context should note that other one dimensional hopping models with random hopping rates show more complicated oscillatory long time behavior [20, 21]. This feature seems to be related to subdiffusive behavior of long time motion, which in turn implies that the probability distribution of $p(j, j')$ puts nonnegligible weight on arbitrarily small hopping rates [20]. Since for our problem $p(j, j') > p_0$ with $p_0 > 0$, we do not expect

our model to show such behavior, even if the simulation experiments could be extended to much larger times.

5 Conclusions

We here have analyzed the effect of disorder in the local mobility on the reptational motion of a polymer chain. Our results led us to consider also the motion of a chain through a regular obstacle lattice of larger lattice constant ($\ell_1 = 2$). In this latter case the chain clearly has to move by the standard reptation mechanism, and our quantitative analysis results in a blob picture: we see reptation of a coarse grained chain. The existence of the blobs shows up in enlarged initial effects, which can be traced back to local motion perpendicular to the tube, and also in the values taken by the parameters ρ_0 and $1/\tau$. These values are larger than their counterparts found for the dense regular obstacle lattice ($\ell_1 = 1$). Since ρ_0 measures the number of mobile entities per segment and $1/\tau$ is related to the relaxation time of a segment, the increase of these parameters indicates the existence of internal degrees of freedom of the effective segments, which build up the coarse grained chain.

Turning now to our simulation results for diluted lattices we note that for dilutions $q \leq 0.6$ they look most similar to the results for the ordered lattices. The correspondence is so close that the same mechanisms must be at work in the two cases. Our quantitative analysis supports this view, in particular since the parameters extracted from the fit yield an internally consistent blob picture. We conclude that reptation is stable against kinematic disorder, at least as long as the disorder configuration percolates through the system. This, together with the validity of the blob concept, is our central result.

Our analysis reveals that it needs chains of $N_t \gtrsim 20$ effective segments to clearly show the qualitative signatures of reptation, like the structure in the motion of the central segment relative to the center of mass (compare Fig. 4b). To unambiguously identify intermediate power laws it even needs larger values $N_t \gtrsim 100$. It thus is not surprising that our data for dilutions $q \geq 0.7$, close to and beyond the percolation threshold of the obstacles, only show first indications of reptational behavior. According to our rough estimates the blobs are so large that the effective chains are of lengths $N_t \lesssim 10$. Still, the overall tendency of the data suggests that the dynamics of the chain does not change qualitatively near the percolation threshold. (See, in particular, Fig. 5)

Of the disorder effects enumerated in the introduction we here included those features which are present both in a melt and in a gel. In a gel in addition entropic and energetic trapping will be present, and this seriously may change the chain dynamics. Indeed, typical results found in the literature [6, 10] show that disorder resulting in points i)-iii) of our list, seriously slows down the chain dynamics and may destroy reptational behavior. In view of our results this must be due to entropic trapping. In a melt there exists no entropic traps, and only a slow relaxation of the environment is to be considered. As we argued

in the introduction we expect this to only enlarge the effective blob size, but not to change the qualitative results. It then is of interest to compare our results to typical simulation results for melts. A particular extensive work has been published by Kremer and Grest [8]. These authors used an off lattice molecular dynamics algorithm to simulate melts of chains up to $N = 400$. Their data for the motion of individual segments look quite similar to our data for short effective chains. Indeed, using a number of different criteria the authors extracted a blob size $n_B \approx 35$, so that the longest chain explicitly analyzed, $N = 200$, consists of only about six blobs. This is completely compatible with the value $\mathcal{R}_{e/m}^{[\max]}(N = 150) \approx 2.9$, which can be extracted from Figure 11a of [8]. Furthermore in the light of our results it explains why the characteristic structure of $g_2(\frac{N}{2}, N, t)$ was not observed, and it is completely compatible with the intermediate effective exponents, which can be extracted from the plots given. In summary, the results of our work are completely compatible with these previous results for melts.

This work was supported by the Deutsche Forschungsgemeinschaft, SFB “Unordnung und grosse Fluktuationen”. Furthermore financial support of UE by the Dutch research foundation NWO and by the EU-TMR-network “Patterns, Noise and Chaos” is gratefully acknowledged.

Appendix A: Analytical reptation results [16]

A.1 Central segment

We write

$$\begin{aligned} \langle (r_{N/2}(t) - \mathbf{r}_{N/2}(0))^2 \rangle &= g_i \left(\frac{N}{2}, N, t \right) \\ &= g_i \left(\frac{N}{2}, N, t \right) + g_r \left(\frac{N}{2}, N, t \right), \end{aligned} \quad (\text{A.1})$$

where g_i represents the motion in the initial tube and g_r is the tube renewal contribution. g_i can be evaluated rigorously to yield

$$\begin{aligned} g_i \left(\frac{N}{2}, N, t \right) &= 2\ell_B^2 \left(\ell_s^2 \rho_0 \frac{1}{\pi} A_1 \left(\frac{N}{2}, t \right) \right)^{1/2} \\ &\times \left[1 - F_1 \left(4\rho_0 A_1 \left(\frac{N}{2}, t \right) \right) \right], \end{aligned} \quad (\text{A.2})$$

where

$$A_1(j, t) = \frac{\hat{t}}{N} + \frac{N}{3} - \frac{1}{2} + \frac{1}{6N} - \left(1 - \frac{1}{N}\right) j + \frac{j^2}{N} - \frac{1}{2N} \sum_{k=1}^{N-1} \alpha_k^t \frac{\cos^2\left(\frac{\pi k}{N}\left(j + \frac{1}{2}\right)\right)}{\sin^2\left(\frac{\pi k}{2N}\right)}. \quad (\text{A.3})$$

$$\alpha_k = 1 - 4p \sin^2\left(\frac{\pi k}{2N}\right) \quad (\text{A.4})$$

$$F_1(z) = \frac{1}{2\sqrt{\pi}} \int_0^z dx x^{-3/2} e^{-x} \left(\left(1 - \frac{x}{z}\right)^{-1/2} - 1 \right) - \frac{1}{2\sqrt{\pi}} \Gamma\left(-\frac{1}{2}, z\right). \quad (\text{A.5})$$

Here $\Gamma(\alpha, z)$ denotes the incomplete Γ -function. Compared to [16] we in equation (A.2) and in the results given below have made the dependence on the segment size ℓ_B of the reptating chain explicit. The spared length ℓ_s and the density of particles ρ_0 are defined relative to ℓ_B .

The tube renewal contribution g_r can be evaluated only approximately. Our result reads

$$g_r\left(\frac{N}{2}, N, t\right) = 2\ell_B^2 \ell_s \overline{n_{\max}(t)} \times \int_0^\infty dz z \left\{ G\left(z + \frac{N}{2\ell_s} \overline{n_{\max}(t)}^{-1}, 0, -a\left(\frac{N}{2}, t\right)\right) + G\left(z + \frac{N}{2\ell_s} \overline{n_{\max}(t)}^{-1}, \frac{\left(\frac{4}{\pi}\rho_0 A_1\left(\frac{N}{2}, t\right)\right)^{1/2}}{\overline{n_{\max}(t)}}, a\left(\frac{N}{2}, t\right)\right) \right\} \quad (\text{A.6})$$

$$a(j, t) = (A_1(0, t)A_1(j, t))^{-1/2} \times \left[\frac{\hat{t}}{N} + \frac{N}{3} - \frac{1}{2} + \frac{1}{6N} + \frac{j^2}{2N} - \left(1 - \frac{1}{2N}\right) j - \frac{1}{2N} \sum_{k=1}^{N-1} \alpha_k^t \frac{\cos\left(\frac{\pi k}{2N}\right) \cos\left(\frac{\pi k}{N}\left(j + \frac{1}{2}\right)\right)}{\sin^2\left(\frac{\pi k}{2N}\right)} \right] \quad (\text{A.7})$$

$$G(z, b, a) = \frac{1}{\pi} (1 - 2ab + b^2)^{-1/2} \frac{1 - ab}{1 - 2ab} \times \exp\left[-\frac{z^2}{\pi}(1 - 2ab + b^2)^{-1}\right] \times \operatorname{erfc}\left(\frac{z}{\sqrt{\pi(1 - a^2)}} \frac{b - a}{(1 - 2ab + b^2)^{1/2}}\right) - \frac{a}{\pi}(1 - 2ab)^{-1} \exp\left[-4a^2 \frac{z^2}{\pi}\right] \times \operatorname{erfc}\left(\frac{1 - 2a^2}{\sqrt{\pi(1 - a^2)}}\right). \quad (\text{A.8})$$

$\overline{n_{\max}(t)}$ is given in equation (A.11), below. (We must apologize for an error of sign in Eq. (5.96) of [16].)

For the cubic invariant \hat{g}_1 (Eq. (2.5)) we only have evaluated the contribution inside the tube. The result reads

$$\hat{g}_1\left(\frac{N}{2}, N, t\right) = \ell_B^2 \left(2\ell_s^2 \rho_0 A_1\left(\frac{N}{2}, t\right)\right)^{1/2}. \quad (\text{A.9})$$

A.2 End segments

The motion of the end segment can be written as

$$g_1(0, N, t) = 2\ell_B^2 \ell_s \overline{n_{\max}(t)}, \quad (\text{A.10})$$

where $\overline{n_{\max}(t)}$ gives the maximal excursion of the chain end into the original tube within time interval t . It can be evaluated only approximately, and we use an approximation based on random walk theory:

$$\overline{n_{\max}(t)} = \sqrt{\frac{\rho_0}{\pi}} \sum_{s=1}^t \frac{1}{s} A_1(0, s)^{1/2} [1 - F_1(4\rho_0 A_1(0, s))]. \quad (\text{A.11})$$

The functions A_1 and F_1 are given above.

References

1. P.G. de Gennes, *J. Chem. Phys.* **55**, 572 (1971).
2. M. Doi, S.F. Edwards, *The Theory of Polymer Dynamics* (Clarendon Press, Oxford, 1986).
3. B.H. Zimm, O. Lumpkin, *Macromol.* **26**, 226 (1993).
4. S.J. Hubert, M. Krzywinski, I. L'Heureux, G.W. Slater, *Macromol.* **31**, 181 (1998).
5. A. Kolinski, J. Skolnick, R. Yaris, *J. Chem. Phys.* **86**, 1567 and 7164 (1987).
6. M. Muthukumar, A. Baumgärtner, *Macromol.* **22**, 1937 and 1941 (1989).
7. M. Deutsch, T.L. Madden, *J. Chem. Phys.* **91**, 3252 (1989).
8. K. Kremer, G.S. Grest, *J. Chem. Phys.* **92**, 5057 (1990).
9. J.S. Shaffer, *J. Chem. Phys.* **101**, 4205 (1994); *J. Chem. Phys.* **103**, 761 (1995).
10. G.W. Slater, S.Y. Wu, *Phys. Rev. Lett.* **75**, 164 (1995).
11. G.M. Foo, R.B. Pandey, D. Stauffer, *Phys. Rev. E* **53**, 3717 (1996).
12. H. Fujita, *Polymer Solutions* (Elsevier, Amsterdam, 1990).
13. T.P. Lodge, N.A. Rotstein, S. Prager, *Advances Chem. Phys. LXXIX*, edited by Prigogine, Rice (Wiley, 1990).
14. A. Baumgärtner, U. Ebert, L. Schäfer, *J. Stat. Phys.* **90**, 1375 (1998).
15. U. Ebert, *J. Stat. Phys.* **82**, 183 (1996); U. Ebert, A. Baumgärtner, L. Schäfer, *Phys. Rev. E* **53**, 950 (1996).
16. U. Ebert, L. Schäfer, A. Baumgärtner, *Phys. Rev. Lett.* **78**, 1592 (1997); *J. Stat. Phys.* **90**, 1325 (1998).
17. K.E. Evans, S.F. Edwards, *J. Chem. Soc., Faraday Trans.* **2**, 1891 (1981).
18. S. Müller (private communication).
19. R. Zwanzig, *J. Stat. Phys.* **28**, 127 (1982).
20. J. Bernasconi, W.R. Schneider, *J. Phys. A* **15**, L729 (1983).
21. D. Stauffer (private communication).